A Combined Timing and Frequency Synchronization and Channel Estimation for OFDM

Hlaing Minn, *Member, IEEE,* Vijay K. Bhargava, *Fellow, IEEE,*
and Khaled B. Letaief, *Fellow, IEEE*

Abstract

This paper addresses training signal based combined timing and frequency synchronization and channel estimation for OFDM systems. The proposed scheme consists of two stages. At the first stage, coarse timing and frequency offset estimates are obtained. Based on these estimates, a (coarse) channel response estimate is obtained. The timing and frequency offset estimates at the second stage are obtained by ML realization based on a sliding observation vector. Then ML channel estimation is performed. A means of complexity reduction by an adaptive scheme is also presented. The simulation results show that the proposed combined approach performs quite well and circumvents the problem of mismatch among individual synchronization tasks.

Index Terms

Timing synchronization, Frequency synchronization, Channel estimation, OFDM, maximum likelihood estimation

This paper was presented in part at the IEEE ICC 2004, Paris, France, June 2004.

H. Minn is with the Dept. of Electrical Engineering, University of Texas at Dallas (UTD), (hlaing.minn@utdallas.edu). V. K. Bhargava is with the Dept. of Electrical & Computer Engineering, University of British Columbia. K. B. Letaief is with the Dept. of Electrical & Electronic Engineering, Hong Kong University of Science & Technology. This work was supported in part by the School of Engineering and Computer Science at UTD, in part by the Natural Sciences and Engineering Research Council of Canada, and in part by the Hong Kong Telecom Institute of Information Technology.

I. INTRODUCTION

Most of the methods for synchronization and channel estimation address either synchronization or channel estimation [1]-[10], but do not consider both jointly. However, errors in synchronization can affect channel estimation and vice versa [11][12]. This paper presents a joint channel estimation and synchronization design. In [13], we developed a combined approach in an ad-hoc manner. This paper presents a more-theoretical combined approach using a maximum-likelihood principle with a sliding observation vector (SOV-ML). The method from [13] would not be applicable to a repetitive training signal composed of several identical parts (e.g., IEEE 802.11a preamble) since it is not equipped with a mechanism to handle possible large timing offsets which can easily occur with repetitive training signals. This paper considers a repetitive training signal and presents a novel mechanism to deal with possible large timing offsets in the combined approach. This paper also provides theoretical performance analysis which reveals impact of error from one task on the performance of another task while [13] did not. This theoretical performance measure could be quite useful, for example, in designing training signals.

In addition, a combined approach has the following advantages. The performance can be improved by iterating between synchronization and channel estimation - using information in one for the other. Practical issues such as choices of observation intervals, algorithm parameter setting, and complexity reduction approaches can be addressed more efficiently. Physical layer adaptation on the synchronization and channel estimation can be more flexibly and efficiently performed. The reason for these advantages lies in the information passing from one task to the other by which the above adaptation and performance improvement are accomplished.

The rest of the paper is organized as follows. Section II describes the system considered and Section III details the proposed synchronization and channel estimation. Performance analyses are presented in Section IV. Simulation results are discussed in Section V, and conclusions are given in Section VI.

II. SYSTEM DESCRIPTION

The complex baseband samples of an OFDM symbol, at the sampling rate $1/T$ (N times sub-carrier spacing), are given by

$$s(k) = \frac{1}{\sqrt{N}} \sum_{n=0}^{N-1} c_n \; e^{j2\pi kn/N}, \;\; -N_g \leq k \leq N-1 \tag{1}$$

where c_n is modulated data (zeros for null sub-carriers), N is the number of inverse Fast Fourier Transform (IFFT) points (same as the total number of sub-carriers), N_g is the number of cyclic prefix (CP) samples and $j = \sqrt{-1}$. We use a training symbol consisting of $P+1$ identical parts. Each part contains M samples and can be generated by (1) with N replaced by M. When $PM = N$, the training

signal can be generated by (1) where $\{c_n\}$ for $n \in \mathcal{J} \equiv \{lP : l = 0, 1, \ldots, M-1\}$ are known pilots (e.g. BPSK-modulated pseudo-noise sequence of length M) and $\{c_n\}$ for $n \notin \mathcal{J}$ are zeros. The first identical part with the time indexes $[-M, -M+1, \ldots, -1]$ can be considered as the CP. This type of repetitive training signal (e.g. preambles from IEEE 802.11a, 802.16a) facilitates simple, low-complexity coarse timing and frequency offset estimation by means of correlation among identical parts. It provides the coarse timing estimation with a robustness to frequency offset. It also gives the coarse frequency offset estimation some robustness against timing offsets and channel dispersion.

Consider a frequency selective multipath fading channel characterized by the sample-spaced CIR

$$h(k) = e^{j\phi} \sum_l h_l \; p(kT - \tau_l - t_0), \; k = 0, \; 1, \; \ldots, \; K-1 \tag{2}$$

where $p(t)$ is the combined response of transmit and receive filters, t_0 is a delay to make the filter response causal, $\{h_l\}$ are complex path gains, $\{\tau_l\}$ are the path delays, ϕ is an arbitrary carrier phase and K is the effective maximum channel delay spread in samples. The training signal is designed such that $M > K$, similar to $N_g > K$ for OFDM data symbols. In the presence of a normalized (by the sub-carrier spacing) frequency offset v and a timing offset ε (assuming a perfect sampling clock and no oscillator phase noise), the length-$(\gamma + PM = N')$ received observation vector is given by

$$\boldsymbol{r}(\varepsilon) = e^{j2\pi\varepsilon v/N} \boldsymbol{W}(v) \cdot \boldsymbol{S}(\varepsilon) \cdot \boldsymbol{h} + \boldsymbol{n}(\varepsilon) \tag{3}$$

where γ is an integer given by $0 \le \gamma \le M - K + 1$ and

$$\boldsymbol{r}(\varepsilon) \triangleq [r(\varepsilon - \gamma) \; r(\varepsilon - \gamma + 1) \; \ldots \; r(\varepsilon + PM - 1)]^T \tag{4}$$

$$\boldsymbol{h} \triangleq [h(0) \; h(1) \; \ldots \; h(K-1)]^T \tag{5}$$

$$\boldsymbol{W}(v) \triangleq \mathrm{diag}\{e^{j2\pi(-\gamma)v/N}, e^{j2\pi(-\gamma+1)v/N}, \; \ldots, \; e^{j2\pi(PM-1)v/N}\} \tag{6}$$

$$\boldsymbol{n}(\varepsilon) \triangleq [n(\varepsilon - \gamma) \; n(\varepsilon - \gamma + 1) \; \ldots \; n(\varepsilon + PM - 1)]^T \tag{7}$$

$$\boldsymbol{S}(\varepsilon) \triangleq [\boldsymbol{s}(\varepsilon - \gamma) \; \boldsymbol{s}(\varepsilon - \gamma + 1) \; \ldots \; \boldsymbol{s}(\varepsilon + PM - 1)]^T \tag{8}$$

$$\boldsymbol{s}(m) \triangleq [s(m) \; s(m-1) \; \ldots \; s(m - K + 1)]^T. \tag{9}$$

In the above equations, $\{n(k)\}$ are independent and identically distributed, zero-mean complex Gaussian noise samples with variance σ_n^2. Note that $s(k)$ is a training sample if $k \in [-M, PM - 1]$ and a data sample if $k \ge PM$. For $k < -M$, $s(k)$ is just zero for a burst-transmission mode and could be a data sample for a continuous-transmission mode. Fig. 1 depicts the training symbol structure and different lengths of the received signal vectors (and corresponding reasons) used in different tasks of the proposed approach. More details will be discussed in related sections.

III. Maximum Likelihood-based Synchronization and Channel Estimation

This section presents the maximum likelihood method for synchronization and channel estimation. For a received observation vector $\boldsymbol{r}(\varepsilon)$ and parameters ε, v and $\boldsymbol{h}$, the likelihood function is given by

$$\Lambda(\boldsymbol{r}(\tilde{\varepsilon});\tilde{\varepsilon},\tilde{v},\tilde{\boldsymbol{h}}) = \frac{1}{(\pi\sigma_n^2)^{N'}} \cdot \exp\{-\frac{1}{\sigma_n^2} \parallel \boldsymbol{r}(\tilde{\varepsilon}) - \boldsymbol{W}(\tilde{v})\boldsymbol{S}\tilde{\boldsymbol{h}} \parallel^2\} \tag{10}$$

where $\tilde{x}$ is a trial value of x and $\|\cdot\|^2$ is the vector norm-square. The ML estimation of ε, v, and $\boldsymbol{h}$ can be obtained as

$$(\hat{\varepsilon},\hat{v},\hat{\boldsymbol{h}})_{\mathrm{ML}} = \arg\max_{\tilde{\varepsilon},\tilde{v},\tilde{\boldsymbol{h}}} \Lambda(\boldsymbol{r}(\tilde{\varepsilon});\tilde{\varepsilon},\tilde{v},\tilde{\boldsymbol{h}}). \tag{11}$$

The above ML estimation uses a sliding observation vector (SOV) $\boldsymbol{r}(\tilde{\varepsilon})$ where $\tilde{\varepsilon}$ is a trial timing point. We adopt an approach of iterating between the channel estimation and synchronization passing information back and forth. Given a CIR estimate $\hat{\boldsymbol{h}}$, the ML estimates of the timing point and the normalized carrier frequency offset, denoted by $\hat{\varepsilon}$ and $\hat{v}$ respectively, are then given by

$$(\hat{\varepsilon},\hat{v})_{\mathrm{ML}} = \arg\min_{\tilde{\varepsilon},\tilde{v}} \mathcal{V}(\boldsymbol{r}(\tilde{\varepsilon});\hat{\boldsymbol{h}},\tilde{\varepsilon},\tilde{v}) \tag{12}$$

where

$$\mathcal{V}(\boldsymbol{r}(\tilde{\varepsilon});\hat{\boldsymbol{h}},\tilde{\varepsilon},\tilde{v}) = \boldsymbol{r}^H(\tilde{\varepsilon})\boldsymbol{r}(\tilde{\varepsilon}) - 2\cdot\Re[\boldsymbol{r}^H(\tilde{\varepsilon})\boldsymbol{W}(\tilde{v})\boldsymbol{S}\hat{\boldsymbol{h}}] + \hat{\boldsymbol{h}}^H\boldsymbol{S}^H\boldsymbol{S}\hat{\boldsymbol{h}} \tag{13}$$

and $(\ )^H$ represents the Hermitian Transpose operation. Depending on the given set of parameters ($(\hat{\boldsymbol{h}},\tilde{\varepsilon})$ or $\tilde{\varepsilon}$ or $\hat{\boldsymbol{h}}$), the corresponding metrics to be minimized are respectively given by

$$\mathcal{V}_{|(\hat{\boldsymbol{h}},\tilde{\varepsilon})}(\boldsymbol{r}(\tilde{\varepsilon});\tilde{v}) \triangleq -2\cdot\Re[\boldsymbol{r}^H(\tilde{\varepsilon})\boldsymbol{W}(\tilde{v})\boldsymbol{S}\hat{\boldsymbol{h}}] \tag{14}$$

$$\mathcal{V}_{|\tilde{\varepsilon}}(\boldsymbol{r}(\tilde{\varepsilon});\hat{\boldsymbol{h}},\tilde{v}) \triangleq \mathcal{V}_{|(\hat{\boldsymbol{h}},\tilde{\varepsilon})}(\boldsymbol{r}(\tilde{\varepsilon});\tilde{v}) + \hat{\boldsymbol{h}}^H\boldsymbol{S}^H\boldsymbol{S}\hat{\boldsymbol{h}} \tag{15}$$

$$\mathcal{V}_{|\hat{\boldsymbol{h}}}(\boldsymbol{r}(\tilde{\varepsilon});\tilde{\varepsilon},\tilde{v}) \triangleq \boldsymbol{r}^H(\tilde{\varepsilon})\ \boldsymbol{r}(\tilde{\varepsilon}) + \mathcal{V}_{|(\hat{\boldsymbol{h}},\tilde{\varepsilon})}(\boldsymbol{r}(\tilde{\varepsilon});\tilde{v}) \tag{16}$$

$$\mathcal{V}(\boldsymbol{r}(\tilde{\varepsilon});\hat{\boldsymbol{h}},\tilde{\varepsilon},\tilde{v}) = \mathcal{V}_{|\hat{\boldsymbol{h}}}(\boldsymbol{r}(\tilde{\varepsilon});\tilde{\varepsilon},\tilde{v}) + \hat{\boldsymbol{h}}^H\boldsymbol{S}^H\boldsymbol{S}\hat{\boldsymbol{h}}. \tag{17}$$

For complexity reduction, we consider two stages namely coarse estimation and fine estimation. First, coarse timing estimation and coarse frequency offset estimation are carried out. Then based on the coarse timing and frequency offset estimates, estimation of channel impulse response (CIR) required in (12) is performed. Next, fine timing and frequency offset estimation is proceeded based on SOV-ML estimation in (12). To account for possible large coarse timing offsets, the fine stage (the CIR estimation and the fine timing and frequency offset estimation) can be equipped with a timing ambiguity resolution mechanism. The fine stage can be iterated for further improvement but the timing ambiguity resolution is no longer required then. For further complexity reduction, the ambiguity resolution can be implemented adaptively where it is not performed if the channel is in good conditions. Since timing metric reflects channel condition, it can be used to decide if ambiguity resolution is necessary. Finally, after obtaining fine timing and frequency offset estimates, sub-carrier frequency response estimation is performed.

A. Coarse Timing and Frequency Estimation

This subsection describes the correlation-based coarse synchronization. We use the following normalized autocorrelation function as our sync detection metric (to detect the presence of training symbol) as well as the coarse timing metric (to find the start of FFT window):

$$\mathcal{C}(\boldsymbol{r}(k), M) \triangleq \frac{(P+1)\left|\sum_{i=-M}^{PM-M-1} r^*(k+i)\cdot r(k+M+i)\right|}{P \ \parallel \boldsymbol{r}(k) \parallel^2}. \tag{18}$$

The coarse timing point ε_c is then advanced by some amount λ_c (> 0). The advantage of timing advancement and the best choice of λ_c are discussed in [13] [14]. We use the following coarse frequency offset estimator

$$\hat{v}_c = \frac{N}{2\pi M} \ \text{angle}\{ \sum_{k=0}^{M-1}\sum_{p=0}^{P-2} r^*(k+p\cdot M+\varepsilon_c)\cdot r(k+p\cdot M+M+\varepsilon_c) \ \} \tag{19}$$

where the estimation range is $-\frac{N}{2\ M} < \hat{v}_c \leq \frac{N}{2\ M}$. Due to space limitation, detailed description on the coarse synchronization is referred to [12].

B. Fine Timing and Frequency Estimation

This subsection presents the maximum likelihood method for fine synchronization. The ML estimates $(\varepsilon_f, \hat{v}_f)_{|(\varepsilon_c,\hat{v}_c)}$, based on the coarse estimates $(\varepsilon_c, \hat{v}_c)$, can be obtained from (12) as

$$(\varepsilon_f, \hat{v}_f)_{|(\varepsilon_c,\hat{v}_c)} = \arg\min_{(\tilde{\varepsilon},\tilde{v})} \{\mathcal{V}(\boldsymbol{r}(\tilde{\varepsilon}); \hat{\boldsymbol{h}}, \tilde{\varepsilon}, \tilde{v}) \ : \varepsilon_c - T_1 \leq \tilde{\varepsilon} \leq \varepsilon_c + T_2, \ \hat{v}_c - F_1 \leq \tilde{v} \leq \hat{v}_c + F_2\}. \tag{20}$$

Here, the search space is limited to $\varepsilon_c - T_1 \leq \tilde{\varepsilon} \leq \varepsilon_c + T_2$ and $\hat{v}_c - F_1 \leq \tilde{v} \leq \hat{v}_c + F_2$ since ε_c and $\hat{v}_c$ cannot be too much far away from the correct values 0 and v. It also reduces the algorithm's complexity. The accuracy of the coarse estimates and the setting of search ranges in (20) are discussed in Appendix. Equation (20) can be implemented by first finding $\tilde{v}$ that minimizes the metric for each $\tilde{\varepsilon}$, denoted by $\hat{v}_{|\tilde{\varepsilon}}$, and then choosing the pair $(\tilde{\varepsilon}, \hat{v}_{|\tilde{\varepsilon}})$ that has minimum metric, which is denoted by $\mathcal{V}_{(\varepsilon_c,\hat{v}_c)}$. By using (14), an ML estimate of v for a trial timing point $\tilde{\varepsilon}$ is obtained as

$$\hat{v}_{|\tilde{\varepsilon}} = \arg\min_{\tilde{v}} \{\mathcal{V}_{|(\hat{\boldsymbol{h}},\tilde{\varepsilon})}(\boldsymbol{r}(\tilde{\varepsilon}); \tilde{v}) \ : \hat{v}_c - F_1 \leq \tilde{v} \leq \hat{v}_c + F_2\} \tag{21}$$

with the corresponding minimum metric $\mathcal{V}_{|(\hat{\boldsymbol{h}},\tilde{\varepsilon})}(\boldsymbol{r}(\tilde{\varepsilon}); \hat{v}_{|\tilde{\varepsilon}})$. Then, an ML timing estimate is obtained by using (16) as

$$\varepsilon_f = \arg\min_{\tilde{\varepsilon}} \{\mathcal{V}_{|\hat{\boldsymbol{h}}}(\boldsymbol{r}(\tilde{\varepsilon}); \tilde{\varepsilon}, \hat{v}_{|\tilde{\varepsilon}}) \ : \varepsilon_c - T_1 \leq \tilde{\varepsilon} \leq \varepsilon_c + T_2\} \tag{22}$$

and the fine estimates are given by $(\varepsilon_f, \hat{v}_f)$ with $\hat{v}_f = \hat{v}_{|\varepsilon_f}$. The above ML realization requires the knowledge of CIR which should not be affected by timing and frequency offsets. The next section will present how to obtain this CIR.

In the following, we describe the implementation of (21). Define $\hat{\boldsymbol{r}}_{\rm ref} \stackrel{\triangle}{=} \boldsymbol{S}\hat{\boldsymbol{h}}$ whose elements are denoted as $\{\hat{r}_{\rm ref}(k)\}$, where $\hat{\boldsymbol{h}}$ is obtained from (34) used in the chosen set among $\{\varepsilon_i, \hat{v}_c\}$ (or, if at further iteration of the fine stage, it is obtained from (34) with previous ε_f and $\hat{v}_f$). Then, (14) can be realized as

$$\mathcal{V}_{|(\hat{\boldsymbol{h}},\tilde{\varepsilon})}(\boldsymbol{r}(\tilde{\varepsilon});\tilde{v}) = -2 \cdot \Re[\sum_{k=-\gamma}^{PM-1} q(k)\ e^{-j2\pi\tilde{v}k/N}] \tag{23}$$

where $q(k) \stackrel{\triangle}{=} \hat{r}^*_{\rm ref}(k)\ r(\tilde{\varepsilon}+k)$. After obtaining $\{q(k)\}$ for a trial point $\tilde{\varepsilon}$, (21) can be implemented in an iterative way using (23) as follows. Set $F_1 = F_2$, $\hat{v}_0 = \hat{v}_c$, and $\Delta_0 = F_1/J_1$.

for $i = 1:1:J_2$

$\tilde{v}_k = \hat{v}_{i-1} + k \cdot \Delta_{i-1}$

$\hat{v}_i = \arg\min_{\tilde{v}_k} \{\mathcal{V}_{|(\hat{\boldsymbol{h}},\tilde{\varepsilon})}(\boldsymbol{r}(\tilde{\varepsilon});\tilde{v}_k)\ : k = -J_1:1:J_1\}$

$\Delta_i = \xi \cdot \Delta_{i-1}/J_1$

end

$$\hat{v}_{|\tilde{\varepsilon}} = \hat{v}_{J_2}. \tag{24}$$

Depending on the coarse frequency offset estimation performance, the value of F_1 can appropriately (and adaptively) be set for complexity reduction (see Appendix). The parameters (J_1, J_2, ξ) give a trade-off between the accuracy and the complexity of the estimation. Alternatively, (21) can be implemented by FFT and interpolation as in [5] but adaptivity for complexity reduction cannot be performed in this FFT-based approach.

C. Channel Estimation for Fine Synchronization

This subsection discusses how channel estimation information is incorporated into the synchronization. Define

$$\bar{\boldsymbol{s}}(k) \stackrel{\triangle}{=} [s(k)\ s(k-1)\ \ldots\ s(k-M+1)]^T \tag{25}$$

$$\bar{\boldsymbol{S}}(k) \stackrel{\triangle}{=} [\bar{\boldsymbol{s}}(k)\ \bar{\boldsymbol{s}}(k+1)\ \ldots\ \bar{\boldsymbol{s}}(k+PM-1)]^T \tag{26}$$

$$\boldsymbol{g} \stackrel{\triangle}{=} [\boldsymbol{h}^T, \boldsymbol{0}_{1\times K_1}]^T \tag{27}$$

where $\boldsymbol{0}_{1\times K_1}$ is an all-zero row vector of length $K_1 = M-K$. We can observe that $\boldsymbol{S}(\varepsilon)\boldsymbol{h} = \bar{\boldsymbol{S}}(\varepsilon)\boldsymbol{g}$. Then $\boldsymbol{r}(\varepsilon)$ can be expressed as

$$\boldsymbol{r}(\varepsilon) = e^{j2\pi\varepsilon v/N}\boldsymbol{W}(v) \cdot \bar{\boldsymbol{S}}(\varepsilon) \cdot \boldsymbol{g} + \boldsymbol{n}(\varepsilon). \tag{28}$$

From the definitions of (26) and (27), the following equality is observed, for $-K_1 \le \varepsilon \le 0$,

$$\bar{\boldsymbol{S}}(\varepsilon)\boldsymbol{g} = \bar{\boldsymbol{S}}(0)\ \mathcal{I}(\varepsilon)\ \boldsymbol{g} \tag{29}$$

where $\mathcal{I}(\varepsilon)$ is a $(K+K_1)\times(K+K_1)$ permutation matrix with $[\mathcal{I}(\varepsilon)]_{i,l}$ being the $[(i+\varepsilon)mod\ (PM),\ l]$-th element of the $(K+K_1)\times(K+K_1)$ identity matrix. In the following, $\bar{\boldsymbol{S}}(0)$ will be denoted by $\bar{\boldsymbol{S}}$. Note that $\mathcal{I}(\varepsilon)\boldsymbol{g}$ is just a cyclically-shifted version of $\boldsymbol{g}$. Substituting (29) into $\boldsymbol{r}$ and applying the ML principle, at the correct sync parameters $(\varepsilon=0,\hat{v}=v)$, result in

$$\hat{\boldsymbol{g}}(0,v)=(\bar{\boldsymbol{S}}^H\bar{\boldsymbol{S}})^{-1}\bar{\boldsymbol{S}}^H\boldsymbol{W}^H(v)\boldsymbol{r}(0). \tag{30}$$

Applying (30) for $\boldsymbol{r}(\varepsilon_c)$ with v replaced by $\hat{v}_c$ gives

$$\hat{\boldsymbol{g}}(\varepsilon_c,\hat{v}_c)=(\bar{\boldsymbol{S}}^H\bar{\boldsymbol{S}})^{-1}\bar{\boldsymbol{S}}^H\boldsymbol{W}^H(\hat{v}_c)\boldsymbol{r}(\varepsilon_c). \tag{31}$$

The mean of the above estimator, if $\hat{v}_c=v$, is

$$E[\hat{\boldsymbol{g}}(\varepsilon_c,\hat{v}_c)]=e^{j2\pi\varepsilon_c\hat{v}_c/N}\ \mathcal{I}(\varepsilon_c)\ \boldsymbol{g}. \tag{32}$$

From (32), we can observe that $\boldsymbol{g}$ can be estimated if ε_c and $\hat{v}_c$ are known. Since we have $\hat{v}_c$ from the coarse synchronization stage, using an estimate $\hat{\varepsilon}_c$ for ε_c results in an estimate of $\boldsymbol{g}$ based on the pair $(\varepsilon_c,\hat{v}_c)$ as follows:

$$\hat{\boldsymbol{g}}_{|(\varepsilon_c,\hat{v}_c)}=e^{-j2\pi\hat{\varepsilon}_c\hat{v}_c/N}\mathcal{I}^H(\hat{\varepsilon}_c)\ \hat{\boldsymbol{g}}(\varepsilon_c,\hat{v}_c). \tag{33}$$

Let $\{\hat{g}(i):i=0,1,\ldots,K+K_1-1\}$ and $\{\hat{g}_c(i):i=0,1,\ldots,K+K_1-1\}$ denote the elements of $\hat{\boldsymbol{g}}_{|(\varepsilon_c,\hat{v}_c)}$ and $\hat{\boldsymbol{g}}(\varepsilon_c,\hat{v}_c)$, respectively. Then, from (27), we obtain a CIR estimate based on the pair $(\varepsilon_c,\hat{v}_c)$ as

$$\hat{\boldsymbol{h}}(\varepsilon_c,\hat{v}_c)=[\hat{g}(0),\hat{g}(1),\ldots,\hat{g}(K-1)]^T. \tag{34}$$

Note that (31) and (32) hold exactly for $-M+K-1\le\varepsilon_c\le 0$ and approximately (due to the inclusion of non-training samples in the vector $\boldsymbol{r}(\varepsilon)$) for $-M+K-1-K_2\le\varepsilon_c\le -M+K-2$ and $1\le\varepsilon_c\le K_3$, for small $K_2,K_3>0$. Let $-M+K-1-K_2\stackrel{\triangle}{=}-K_4$. Since (31) produces a cyclically-shifted version of a length-M vector $\hat{\boldsymbol{g}}$, the allowable timing offset for the channel estimation is limited to $-K_4\le\varepsilon_c\le K_3$ where $K_3+K_4+1=M$.

The estimate $\hat{\varepsilon}_c$ required in (33) can be obtained as

$$\hat{\varepsilon}_c=\begin{cases} l_{\max} & \text{if } l_{\max}\ge -K_4 \\ M+l_{\max} & \text{otherwise} \end{cases} \tag{35}$$

where

$$l_{\max}\ \stackrel{\triangle}{=}\ \arg\max_{l}\ \{E_h(l,\varepsilon_c)\ :l=0,-1,\ldots,-M+1\} \tag{36}$$

$$E_h(l,\varepsilon_c)\ =\ \begin{cases} \sum_{k=0}^{K-1}|\hat{g}_c((-l+k)_{\mathrm{mod}\ (K+K_1)})|^2 & \text{if } |\hat{g}_c(-l)|>\eta\cdot\max_i\{|\hat{g}_c(i)|\} \\ 0 & \text{otherwise .} \end{cases} \tag{37}$$

Here, η is a threshold parameter for selecting the first tap of the CIR (see [13] for details). Note that (35) can be considered as a further fine-tuning of the coarse timing estimate by means of the CIR estimation

designed to give a cyclically-shifted (due to timing offset) extended CIR estimate. ML estimation in (20) can now be realized for $-K_4 \leq \varepsilon_c \leq K_3$ using (35)-(37) together with (33)(34)(21) and (22).

If $\varepsilon_c < -K_4$, $\hat{\boldsymbol{h}}_{\rm req}(\varepsilon_c, \hat{v}_c)$ required in (20) is given by (34) and (33) with $\hat{\varepsilon}_c$ replaced by $l_{\max}$. However, due to the ambiguity, $\hat{\varepsilon}_c$ will be $M + l_{\max}$ and consequently the estimated channel response would be $\hat{\boldsymbol{h}}(\varepsilon_c, \hat{v}_c) = \hat{\boldsymbol{h}}_{\rm req}(\varepsilon_c, \hat{v}_c)\ e^{-j2\pi M \hat{v}_c/N}$ under no noise condition. Then, (20) would quite likely give a timing point around $-M$ due to the extra factor $e^{-j2\pi M \hat{v}_c/N}$ contained in the channel estimate. Similarly, if $\varepsilon_c > K_3$, (20) would quite likely give a timing point around M. To solve this ambiguity problem, we consider three candidates for the coarse timing point, namely, $\{\varepsilon_i \ : i = -1, 0, 1\}$ with $\varepsilon_i = \varepsilon_c + i \cdot M$. For each set $(\varepsilon_i, \hat{v}_c)$, realizing (20) results in a candidate set of fine estimates $(\varepsilon_f, \hat{v}_f)_i$ together with the corresponding minimum metric $\mathcal{V}_{(\varepsilon_i, \hat{v}_c)}$. The fine estimates are then obtained as

$$(\varepsilon_f, \hat{v}_f) = \underset{(\varepsilon_f, \hat{v}_f)_i}{\arg\min} \{\mathcal{V}_{(\varepsilon_i, \hat{v}_c)} : i = -1, 0, 1\}. \tag{38}$$

Since each candidate ε_i can produce a proper channel estimate if it is within the allowable range, the search window of $\tilde{\varepsilon}$ can be set such that $T_1 = K_3$ and $T_2 = K_4$. By this ambiguity resolution, the allowable coarse timing offset range for realization of (20) is extended to $-M - K_4 \leq \varepsilon_c \leq M + K_3$ which is usually more than sufficient for the SNR of interest (see Appendix). The fine estimation stage can be iterated for further improvement. At this time, ambiguity resolution will no longer be required. The final estimates can be taken from the last iteration or from the iteration with minimum metric.

D. Estimation of Channel Frequency Response

In this subsection, we obtain the maximum likelihood estimate of the frequency-domain channel gains to be used in the equalization. The fine timing point will be most of the time at the correct point and hence, the channel estimation performed then can be based on the length-$(PM + M - K + 1)$ received vector $\boldsymbol{r}$, (i.e., with $\gamma = M - K + 1$), as follows:

$$\hat{\boldsymbol{h}}_f = (\boldsymbol{S}^H \boldsymbol{S})^{-1} \boldsymbol{S}^H \boldsymbol{W}^H(\hat{v}_f) \boldsymbol{r}(\varepsilon_f). \tag{39}$$

If we have knowledge of the number of nontrivial channel taps $\mathcal{K}$, the channel estimation can further be improved by using the $\mathcal{K}$ largest taps out of K estimated taps [9][10]. To account for the occasional occurrence of $\varepsilon_f > 0$ which will cause ISI, the (final) fine timing estimate is advanced by λ_f (> 0) samples. In this case, $\hat{\boldsymbol{h}}_f$ which is obtained above with no timing advancement can be modified as

$$\hat{\boldsymbol{h}}_f(\lambda_f) = e^{-j2\pi \hat{v}_f \lambda_f / N}\ [\boldsymbol{0}_{1\times\lambda_f},\ \hat{\boldsymbol{h}}_f^T]^T. \tag{40}$$

Finally, N-point FFT of $\hat{\boldsymbol{h}}_f(\lambda_f)$ gives the sub-channel frequency response estimates.

IV. Performance Analysis

This section analyzes how errors in one task affect the other. Let $\Delta \boldsymbol{h} = \hat{\boldsymbol{h}} - \boldsymbol{h}$, $\boldsymbol{C}_{\Delta \boldsymbol{h}} = E[\Delta \boldsymbol{h} \Delta \boldsymbol{h}^H]$, $\boldsymbol{y} \triangleq \frac{2\pi}{N} \boldsymbol{\mathcal{W}} \boldsymbol{S} \boldsymbol{h}$ and $\boldsymbol{\mathcal{W}} \triangleq \text{diag}\{-N_g + K - 1, -N_g + K, \ldots, PM - 1\}$. Following the method from [5] and assuming that $E[\Delta h(k)] = 0$, we obtain $E[\hat{v}] = v$ and

$$\text{var}[\hat{v}] \simeq \frac{1}{2} \left\{ \frac{\sigma_n^2}{\boldsymbol{y}^H \boldsymbol{y}} + \frac{\boldsymbol{y}^H \boldsymbol{S} \boldsymbol{C}_{\Delta \boldsymbol{h}} \boldsymbol{S}^H \boldsymbol{y} + \frac{4\pi^2}{N^2} \sigma_n^2 \, \text{trace}\{\boldsymbol{\mathcal{W}} \boldsymbol{S} \boldsymbol{C}_{\Delta \boldsymbol{h}} \boldsymbol{S}^H \boldsymbol{\mathcal{W}}\}}{(\boldsymbol{y}^H \boldsymbol{y})^2} \right\}. \tag{41}$$

Equation (41) indicates that the frequency estimation accuracy depends on the channel response, the training symbol and the channel estimation error. Similarly, the channel estimation MSE, for particular $\Delta v = \hat{v} - v$ and $\boldsymbol{h}$, can be given by

$$\text{MSE}[\hat{h}(k)] \simeq \left[\sigma_n^2 (\boldsymbol{S}^H \boldsymbol{S})^{-1} + \{\boldsymbol{h}\boldsymbol{h}^H - (\boldsymbol{S}^H \boldsymbol{S})^{-1} \boldsymbol{S}^H \boldsymbol{\mathcal{W}}^H (\Delta v) \, \boldsymbol{S} \boldsymbol{h} \boldsymbol{h}^H\} \{\boldsymbol{I} - \boldsymbol{S}^H \boldsymbol{\mathcal{W}} (\Delta v) \boldsymbol{S} (\boldsymbol{S}^H \boldsymbol{S})^{-1}\} \right]_{k,k} \tag{42}$$

which indicates that the channel estimation accuracy depends on the frequency estimation accuracy. The second term, which is caused by the frequency estimation error, also depends on the channel response and the training symbol.

V. Simulation Results and Discussions

The simulation parameters are $N = 64$, $N_g = M = 16$, $P = 4$, $v = 1.6$, $\lambda_c = 4$, $\lambda_f = 2$, QPSK for the uncoded system (without error correction code) and BPSK for the coded system (with a rate 1/2, constraint length 7, convolutional code with an interleaver, both from IEEE 802.11a). We assume a quasi-static Rayleigh fading channel with 8 sample-spaced paths (hence, $K = 8$ and $t_0 = 0$) and a power delay profile of a 3 dB per tap decaying factor. We use $K' = K = 8$ and $\mathcal{K} = 8$ unless stated otherwise. The parameters for (24) and (22) are $F_1 = 0.1$, $J_1 = 10$, $J_2 = 5$, $\xi = 2$, $T_1 = K_3 = 4$ and $T_2 = K_4 = 11$. One packet contains one training symbol and 5 data symbols. The results are obtained from 10^5 simulation runs. "Fine^k" denotes the fine stage with k iterations and "Fine (selected)" represents the fine stage where the final estimates are selected from the iteration with the minimum metric among 5 iterations.

A motivation for the combined approach is that errors in one task can affect the other tasks in synchronization and channel estimation. Illustrative results for this fact are referred to [12], due to space limitation. The performance of the ambiguity resolution of the timing offset at the fine synchronization stage is referred to [14]. The performance advantages of the proposed combined approach in terms of timing offset variance, normalized interference power caused by timing offsets, frequency offset estimation MSE, and channel estimation MSE are referred to [12] for the same reason. Fine stage improves all estimation performance substantially. Further iteration at fine stage improves frequency offset and channel

estimation slightly. Further iteration is not necessary for timing estimation since the first-round fine timing estimation is sufficient enough that further iteration could not bring in a noticeable improvement.

In Fig. 2(a), as an overall performance measure, uncoded BER performance curves are presented. The fine stages have considerably better BER performance than the coarse stage. More iterations in the fine stage slightly improve the BER performance especially at moderate and low SNR values. "Fine (selected)" case has a marginally better BER performance than other cases. Fig. 2(a) also presents the BER performance for a packet containing one training symbol and one data symbol (to decouple the frequency-offset-induced accumulated phase offset effect[1] from the estimation performance). The results indicate that the proposed scheme performance is quite close to the case with known sync parameters and known channel response. The performance comparison of the adaptive ambiguity resolution and the non-adaptive ambiguity resolution is referred to [14]. The adaptive approach achieves almost the same BER performance and a substantial complexity reduction gain.

We have evaluated the proposed method with the designed maximum channel delay spread K' and the designed number of the most significant channel taps $\mathcal{K}$ (denoted by "MST" in the figure) different from their actual values. The uncoded BER curves are given in Fig. 2(b). Due to the noise contamination from the extra taps, a slight performance loss is observed. However, a considerable performance improvement over the coarse stage is still achieved.

Fig. 3 presents the coded BER curves together with the corresponding uncoded BER curves. We used a soft-decision Viterbi decoding with the branch metric $\sum_{l=0}^{1} \|Y_{k_l} - \hat{H}_{k_l} C_l\|^2$ where $\{Y_{k_l}\}$ are frequency-offset-compensated received sub-carrier symbols, $\{\hat{H}_{k_l}\}$ are corresponding channel gain estimates, $\{C_l\}$ are sub-carrier modulation symbols, and $\{k_0, k_1\}$ are sub-carrier indices (after de-interleaving) corresponding to the k-th time-instant of the Viterbi algorithm. A significant improvement (much greater than that in the uncoded system) is observed for the fine stages. The second iteration improves the coded BER considerably over the first iteration although its improvement in uncoded BER is marginal.

VI. Conclusions

This paper presented a sliding observation vector based maximum-likelihood combined timing and frequency synchronization and channel estimation method using a repetitive training signal. If not taken into account, errors from one task can affect the other tasks. The proposed combined approach circumvents the problem of mismatch among different individual tasks, i.e. the problem of high sensitivity of one

[1]In practice, the accumulated phase and the time-varying channel effects are taken care of by transmitting pilot tones regularly.

task to errors in other tasks. The fine stage of the proposed method improves the error performance considerably for the uncoded system and significantly for the coded system over the coarse stage.

APPENDIX

This appendix presents coarse timing and frequency offset estimation performance which can be used in designing the combined approach (e.g., in setting the search range of fine frequency offset estimation).

Fig. 4(a) plots probability mass function of coarse timing offset (with $\lambda_c = 4$) obtained by simulation where the threshold for the sync detection metric $\mathcal{C}^2(\boldsymbol{r}(k), M)$ was 0.2. The allowable timing offset estimation range of the fine stage without ambiguity resolution is $-12 < \hat{\varepsilon}_c < 5$ and that with ambiguity resolution is $-28 < \hat{\varepsilon}_c < 21$. The proposed coarse timing estimation with the ambiguity resolution always gives timing point within the allowable range for SNR of practical interest (> 5 dB). Probability mass function of coarse timing offset can easily be obtained by computer simulation within a short time interval, hence one can easily check, for different system parameters, whether further ambiguity resolution is needed or not. If ambiguity resolution is not desirable due to complexity concern, a longer training signal can be used and the training length can be designed based on out-of-range probabilities.

Regarding the performance of coarse frequency offset estimation in (19), the coarse frequency offset estimation error is given by

$$\Delta v_c = \hat{v}_c - v = \frac{N}{2\pi M} \text{ angle}\{Z\} \tag{43}$$

where

$$Z = \sum_{k=0}^{M-1} \sum_{p=0}^{P-2} r^*(k + p \cdot M) \cdot r(k + p \cdot M + M) \; e^{-j2\pi v M/N}. \tag{44}$$

By central limit theorem, Z can be approximated as a complex Gaussian random variable. Then the probability density function of θ = angle$\{Z\}$ can be calculated as

$$f_\theta(\theta) = \frac{1}{2\pi} e^{-\frac{\mu_Z^2}{\sigma_Z^2}} + \frac{\mu_Z \cos(\theta)}{2\sqrt{\pi}\sigma_Z} e^{-\frac{\mu_Z^2 \sin^2(\theta)}{\sigma_Z^2}} \text{erfc}(-\frac{\mu_Z \cos(\theta)}{\sigma_Z}) \tag{45}$$

where erfc($\cdot$) is the complementary error function. If the allowable range of coarse frequency offset estimation error is $-F_1 \leq \Delta v_c \leq F_1$, then $P_o(F_1)$, the probability of the out-of-range frequency offset estimation error is given by

$$P_o(F_1) = \text{Prob}[|\Delta v_c| > F_1] = 1 - \int_{-2\pi M F_1/N}^{2\pi M F_1/N} f_\theta(\theta) d\theta \tag{46}$$

$$= 1 - \frac{2MF_1}{N} \; e^{-\Gamma^2} - \int_{-2\pi M F_1/N}^{2\pi M F_1/N} \frac{\Gamma}{2\sqrt{\pi}} \cos(\theta) e^{-\Gamma^2 \sin^2(\theta)} \text{erfc}(-\Gamma \cos(\theta)) d\theta \tag{47}$$

where $\Gamma = \frac{\mu_Z}{\sigma_Z}$ = $\sqrt{\frac{(N-M)\cdot \text{SNR}_s^2}{2\cdot \text{SNR}_s + 1}}$ is a function of snap-shot received SNR, $\text{SNR}_s = \frac{\sum_{k=0}^{N-M-1} |x(k)|^2}{(N-M)\sigma_n^2}$, where $x(k)$ is channel output training sample defined by $r(k) = x(k)e^{j2\pi vk/N} + n(k)$.

In Fig. 4(b) the probability of the out-of-range frequency offset estimation error is plotted for several SNR_s. If SNR_s is too low, the signal will not be detected by the receiver. Hence, in designing the search range using $P_o(F_1)$, it is not necessary to use a very low SNR_s. In our simulation, we used $F_1 = 0.1$ and the simulation results presented in Section V show that the fine frequency offset estimation performance is satisfactory for all considered average SNR values from 5 dB to 25 dB. Hence, one can design the search range of fine frequency offset estimation by choosing minimum F_1 which gives $P_o(F_1) < 10^{-3}$ at SNR_s = 10 dB (or 5 dB for a more conservative design). If complexity reduction is desired, we can use an adaptive setting of the fine frequency offset estimation search range. The different search ranges for different ranges of SNR_s can be obtained from $P_o(F_1)$. Since the timing metric reflects a measure of SNR_s [14], we can use it for a table-lookup adaptive search range selection.

REFERENCES

[1] M. Speth, F. Classen and H. Meyr, "Frame synchronization of OFDM systems in frequency selective fading channels," *IEEE VTC*, May 1997, pp. 1807-1811.

[2] D. Landström, S. K. Wilson, J.J. van de Beek, P. Ödling and P. O. Börjesson, "Symbol time offset estimation in coherent OFDM systems," *IEEE ICC*, June 1999, pp. 500-505.

[3] B. Yang, K. B. Letaief, R. S. Cheng and Z. Cao, "Timing recovery for OFDM transmission," *IEEE Journal on Selected Areas in Commun.*, Vol. 18, No. 11, Nov. 2000, pp. 2278-2290.

[4] M. Luise and R. Reggiannini, "Carrier frequency acquisition and tracking for OFDM systems," *IEEE Trans. Commun.*, Vol. 44, No. 11, Nov. 1996, pp. 1590-1598.

[5] M. Morelli and U. Mengalli, "Carrier-frequency estimation for transmissions over selective channels," *IEEE Trans. Commun.*, Vol. 48, No. 9, Sept. 2000, pp. 1580-1589.

[6] J-J. van de Beek, M. Sandell and P.O. Börjesson, "ML estimation of time and frequency offset in OFDM systems" *IEEE Trans. Signal Proc.*, Vol. 45, No. 7, July 1997, pp. 1800-1805.

[7] T. M. Schmidl and D. C. Cox, "Robust frequency and timing synchronization for OFDM," *IEEE Trans. Commun.*, Vol. 45, No. 12, Dec. 1997, pp. 1613-1621.

[8] O. Edfors, M. Sandell, J.-J. van de Beek, S. K. Wilson and P. O. Borjesson, "OFDM channel estimation by singular value decomposition," *IEEE Trans. Commun.* Vol. 46, July 1998, pp. 931-939.

[9] Y. Li, L. J. Cimini, Jr., and N. R. Sollenberger, "Robust channel estimation for OFDM systems with rapid dispersive fading channels," *IEEE Trans. Commun.*, Vol. 46, July 1998, pp.902-915.

[10] H. Minn, D.I. Kim, and V. K. Bhargava, "A reduced complexity channel estimation for OFDM systems with transmit diversity in mobile wireless channels," *IEEE Trans. Commun.*, Vol. 50, May 2002, pp.799-807.

[11] M. Speth, S. A. Fechtel, G. Fock and H. Meyr, "Optimum receiver design for wireless broad-band systems using OFDM-Part I," *IEEE Trans. Commun.*, Vol. 47, No. 11, Nov. 1999, pp. 1668-1677.

[12] H. Minn, V.K. Bhargava and K. Ben Letaief, "A Combined Timing and Frequency Synchronization and Channel Estimation for OFDM," *IEEE ICC 2004*, Communications Theory Symposium, pp. 872-876, June 2004.

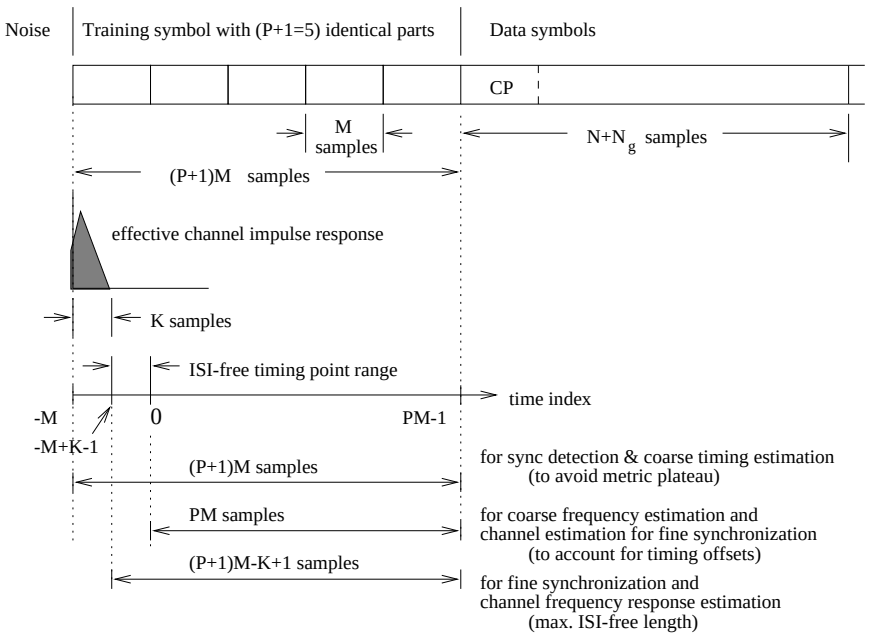

Fig. 1. The training symbol structure and the lengths of received vectors used in different tasks of the proposed approach

[13] H. Minn, V. K. Bhargava and K. Ben Letaief, "A robust timing and frequency synchronization for OFDM systems," *IEEE Trans. Wireless Commun.*, Vol. 2, No. 4, pp. 822-839, July 2003.

[14] H. Minn, V.K. Bhargava and K. Ben Letaief, "Channel estimation assisted improved timing offset estimation," *IEEE ICC 2004*, Communications Theory Symposium, pp. 988-992, June 2004.

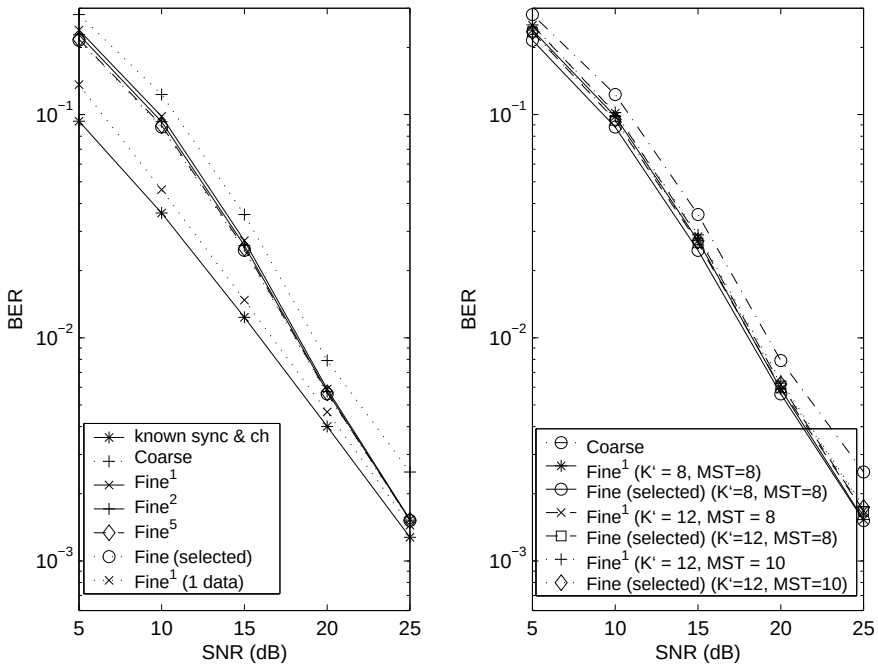

Fig. 2. The uncoded BER performance of the proposed method for: (a) Matched parameters (b) Mismatched parameters

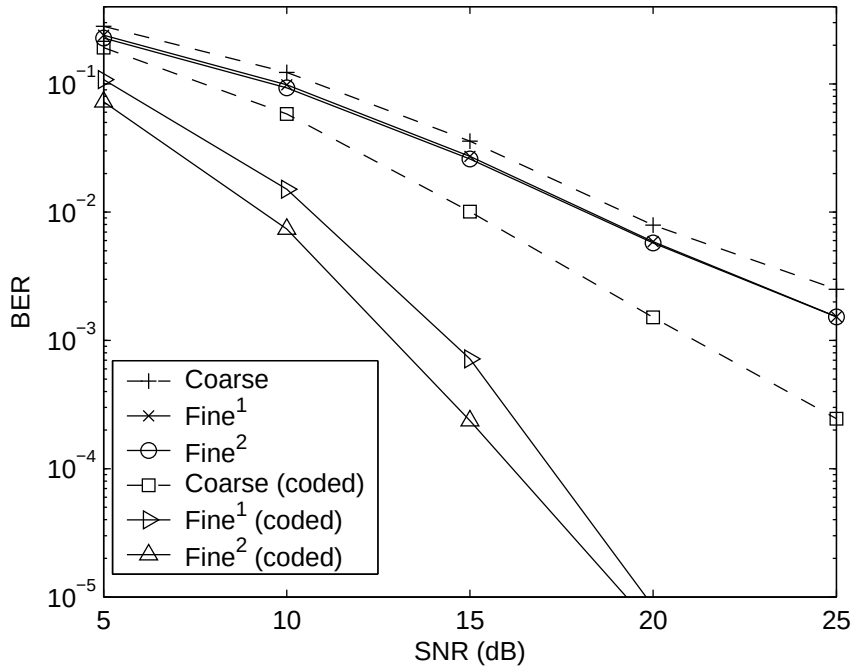

Fig. 3. The coded BER performance improvement of the fine stage over the coarse stage

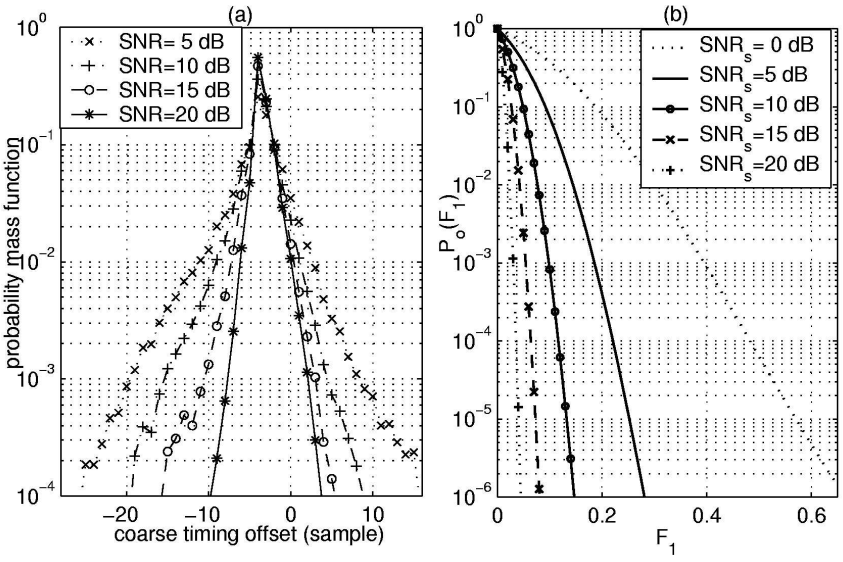

Fig. 4. (a) Probability mass function of coarse timing offset, (b) Out-of-range probability of coarse frequency offset estimation